Chalcogenide Letters Vol. 14, No. 12, December 2017, p. 529 - 537

GAMMA IRRADIATION EFFECTS ON THE LINEAR AND NONLINEAR OPTICAL PROPERTIES OF NONCRYSTALLINE Sb_2S_3 FILMS

S. R. ALHARBI[a*], K. F. A. EL-RAHMAN[b,c]
[a]*Physics Department, Faculty of Sciences, Al Faisaliah, King Abdulaziz University, Jeddah, Saudi Arabia*
[b]*Department of Physics, Faculty of Education, Ain Shams University, Roxy square11757, Cairo, Egypt*
[c]*Department of Physics, Faculty of Science for girls, King Khalid University, Abha, Saudi Arabia*

Sb_2S_3 Noncrystalline Chalcogenide films were synthesized via thermal vapor deposition approach. At room temperature, the intended films were irradiated with absorbed doses 100, 200 and 300 kGy and they have been characterized before and after irradiation by means of diffraction of X-ray. Spectrophotometric measurements were utilized to study the optical parameters for as grown and irradiated Sb_2S_3 films. It is found that a little modification in the fundamental energy band gap occurred while a significant change was occurring in the refractive index spectra. The dispersion of refractive index are modeled in accordance with a Wemple-DiDomenico single-oscillator model. This model is utilized to figure the nonlinear index of refraction (n_2) and third-order nonlinear susceptibility ($\chi^{(3)}$). It is found that $\chi^{(3)}$ and n_2 increased with increasing irradiation doses. This may be explained by the fact that the external gamma irradiation causes an occurrence of defect centers.

(Received October 6, 2017; Accepted December 9, 2017)

Keywords: Chalcogenide; noncrystalline films; optical properties.

1. Introduction

The tendency of radiation sensibility has extraordinarily enhanced throughout the most recent two decades [1-5]. This has turned out to be so, because of the way that ionizing radiations are discovering more applications in a few fields, including industry, medicine, military, research and so on [1-3]. Tragically, all over the place radiation introduction may happen and strict checking of the radiation levels is exceptionally crucial to guarantee the environmental safety for the specialists. To simply check the radiation levels, it is critical to creating novel radiation sensors with the continuous reaction that would start immediately alert sign in the event of crisis [2,3].

Noncrystalline chalcogenide materials are distinguished by the sensibility to the impact of outer factors particularly ionizing radiation. Optical dosimetric taking into account noncrystalline chalcogenide materials can be used for radiation estimations in an extensive variety of assimilated dosages of high-energy ionizing radiation [2,3].

Chalcogenide glass materials particularly antimony trisulphide (Sb_2S_3) have gotten extensive consideration because of its properties, for example, photosensitive, high refractive index, high absorption coefficients ($>10^3$ cm^{-1}), thermoelectric properties, optimum band gap (~ 1.8 eV). However, Sb_2S_3 shows structural change when irradiated by light and by an electron beam [6-9]. Different techniques have been utilized to fabricate Sb_2S_3 films [10-15]. From these techniques, thermal evaporation offering the prospect to adjust the deposition case to get films with particular structural and physical properties [9,10]. The major focus of this research has been on the deposition and characterization of Sb_2S_3 films.

*Corresponding author: srfalharbi@kau.edu.sa

The mechanism of gamma rays interaction with noncrystalline materials fundamentally happens with a method for electronic ionization, electronic excitation and principally atomic separation of the orbital electrons [1]. So, this study concerns on the fabrication of noncrystalline Sb_2S_3 thin films and exploring the changes in their structural and optical characteristics after different doses rate gamma irradiation.

2. Experimental details

Sb_2S_3 thin films were fabricated by thermal vapor deposition method utilizing Edwards E306A coating unit, onto substrates of optic flat quartz, which were beforehand cleaned. For the purpose of obtaining homogeneous fabricated films, the substrate was fixed onto a rotatable holder at a separation of 25 cm over the evaporator. The Sb_2S_3 preparation process was carried out in a vacuum greater than 10^{-4} Pa and the temperature of the substrate has been retained at room temperature. As determined by a quartz crystal thickness monitor and an optical interferometric approach [16], the Sb_2S_3 films thicknesses were 450 nm. The deposition rate was kept nearly fixed to be 3 nm/s. Gamma cell source of ^{60}Co was applied to irradiate the Sb_2S_3 films in the air at ambient temperature. The aggregate doses were altered from 50 to 300 kGy and the rate absorption dose was 800 Gy/h. The films absorbed a series of different integrated doses by exposing it to gamma radiation for a different time.

The X-ray Diffraction (XRD) patterns were recorded with the help of an X'pert Philips diffractometer to identify the structural nature of Sb_2S_3 films. The XRD measurements utilized with a CuKα radiation monochromatic worked at 40 kV and 25 mA. Automatically, the diffraction patterns were done with an examination speed of 2 deg/min. A JASCO V-570 double beam spectrophotometer was used to record the optical transmittance T and reflectance R of the Sb_2S_3 samples detected at vertical incidence and covered the spectral range of 300-1200 nm. The spectra of T and R were done for both as prepared and irradiated Sb_2S_3 samples. The R was measured at vertical incidence with reference of Al mirror.

After rectification the reflectance and absorbance of the substrates, the recorded T and R values are set by the following relation [17,18]

$$T = (I_{ft} / I_q)\,(1 - R_q) \tag{1}$$

I_{ft} is being the light's intensity going through the film-quartz configuration, I_q and R_q are the intensity and the reflectance of the of quartz reference. Moreover, in case of the light reflected from the specimen mirror coming to the detector the intensity is being I_{fr} and that reflected from the reference mirror is I_m, then [17,18]

$$R = (I_{ft} / I_m)\,R_m\,[\,1 + (1 - R_q)^2] - T^2\,R_q \tag{2}$$

where R_m is the reflectance of Al mirror.

At each wavelength, the optical constants (refractive index n and extinction coefficient k) are computed using the rectification values of T and R utilizing a private computer program set up on the following equations [19]:

$$T = \frac{(1-R)^2 e^{-\alpha d}}{1 - R^2 e^{-2\alpha d}} \tag{3}$$

and

$$R = \frac{(n-1)^2 + k^2}{(n+1)^2 + k^2} \tag{4}$$

Here d is the thickness of the film and α is the absorption coefficient which were calculated from the following formula [19]

$$\alpha = \frac{1}{d} \ln\left[\frac{(1-R)^2}{T} + \sqrt{\frac{(1-R)^2}{4T^2} + R^2}\right] \tag{5}$$

Then extinction coefficient k given from [19]

$$\alpha = \frac{4\pi k}{\lambda} \tag{6}$$

Using equation (4), we can compute n from the equation [19]:

$$n = \left(\frac{1+R}{1-R}\right) + \sqrt{\frac{4R}{(1-R)^2} - k^2} \tag{7}$$

Considered that the experimental error for d estimation was ±3% and that for T and R computations was ±1.5%. Then, the experimental error for n was ±2.3% and for k was ±2.

3. Results and discussions

The structural investigation was studied for the as prepared and irradiated Sb_2S_3 films by XRD, which is demonstrated in Fig. 1. This figure indicates that the diffraction from the samples do not show sharp Bragg peaks, which implies that the Sb_2S_3 films lack long range order and it exhibits a broad hump. Also, beneath $2\theta = 20^{\circ}$, there is no diffraction peaks have been observed which implies that the films have loss of medium-range crystalline order. The XRD analysis demonstrates that the films possess the highest level of the noncrystalline state [20,21].

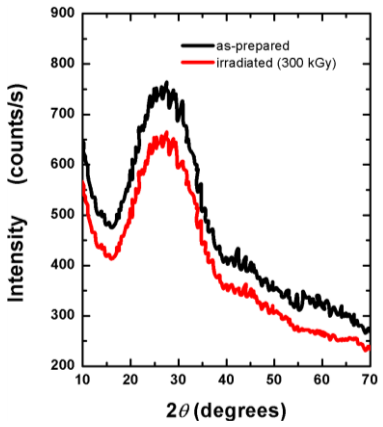

Fig. 1: XRD patterns of as prepared and gamma-irradiated Sb_2S_3 thin films.

The transmittance and reflectance coefficient spectra of the as-prepared as well as gamma-irradiated Sb_2S_3 chalcogenide films are illustrated in Fig. 2. The results unmistakably demonstrate the presence of a major transmission edge isolating the transmission regime from absorption part. The being of this edge in investigated films endorses them as promising optical candidate materials. At shorter wavelengths λ<600 nm, the spectra of T and R suggest the presence of absorption. At longer wavelengths, λ > 600 nm, no light was absorbed or scattered. The given dosage of gamma irradiation moves the transmission edge to longer wavelengths demonstrating that the energy band gap will be diminished with irradiation dosages.

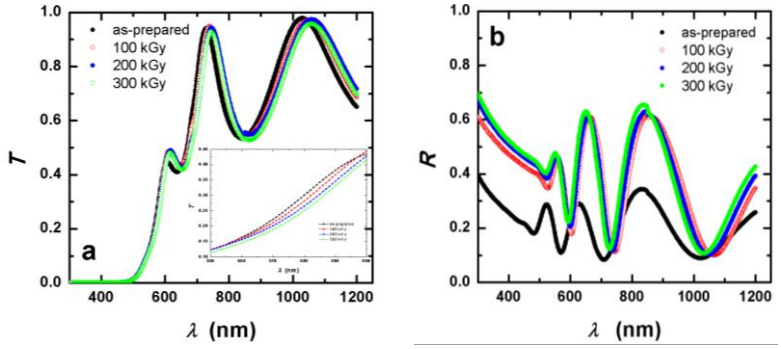

Fig. 2. Transmittance and reflectance spectra for as prepared and irradiated Sb_2S_3 films

The absorption coefficient (α) data are employed to gain information about the electronic transition type and optical energy bandgap E_g through Bardeen's equation [22,23]:

$$(\alpha h\nu)^{r} = B\,(h\nu - E_g \pm E_{ph}) \tag{8}$$

In this equation, B is a constant in regard to the band tailing and electrical conductivity, $h\nu$ is the incident photon energy, E_g is the optical bandgap value, E_{ph} is the phonon energy and r being the power factor of the transition mode. The index r can have different values (2/3 and 2) corresponding to forbidden and allowed direct transitions, respectively, while values (1/3 and ½) corresponding to forbidden and allowed indirect transitions, respectively. Accordingly, the photon energy-$(\alpha h\nu)^{1/2}$ relation of Sb_2S_3 films (presented in Fig. 3) reveals an allowed indirect transition. The hν-axis crossings of the solid lines point to the optical energy gap. Table 1 lists the obtained values of E_g and E_{ph}. The changing in the bandgap values could be ascribed to the spreading of structural disorder and ascending deformities number and structural defects in the crystal-field and structural bonding [24] resulting in exposing Sb_2S_3 films to different doses of gamma radiation. An exponential tail of the optical absorption edge of Sb_2S_3 noncrystalline films points to the existence of localized states, which is normal to be with the indirect transitions in noncrystalline materials. This is a supporting the short range order structure obtained via the XRD.

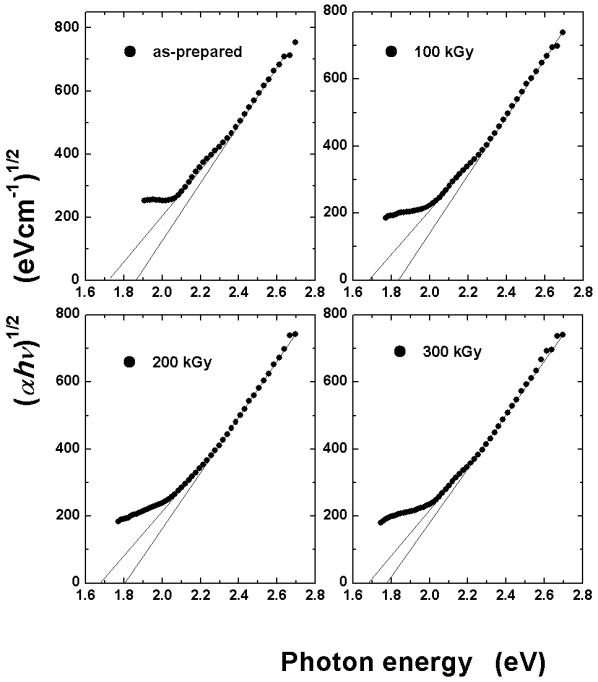

Fig. 3. Dependence of $(\alpha h\nu)^{1/2}$ on photon energy for as prepared and irradiated Sb_2S_3 films

Table 1: The absorption constants for as-prepared and irradiated Sb_2S_3 films

Sample	E_g (eV)	E_{ph} (eV)	E_u (eV)
as-prepared	1.79	0.08	0.386
100 kGy	1.75	0.07	0.341
200 kGy	1.74	0.06	0.339
300 kGy	1.73	0.05	0.328

Fig. 4 illuminates the linear dependence of ln(α) on $h\nu$. The tail width value, E_u, is yielded from inverse of the slope and is listed in Table 1.

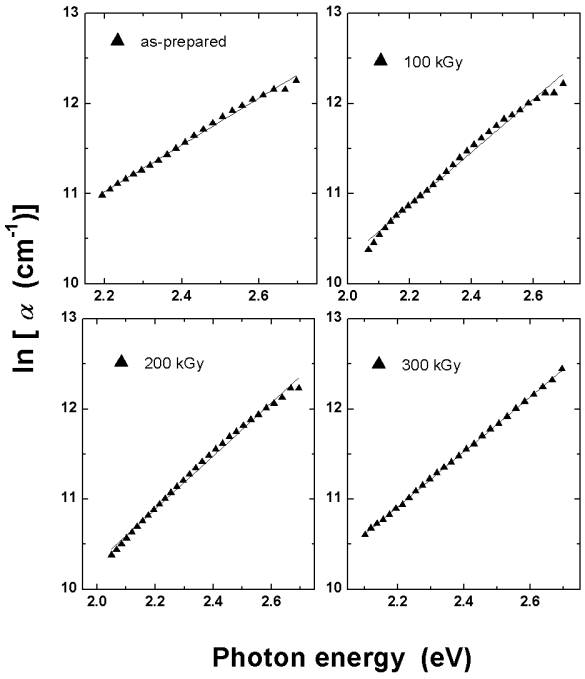

Fig. 4. Spectral reliance of ln(α) on photon energy for as prepared and irradiated Sb_2S_3 films

In optical communications and in designing the devices, an essential part as a critical operator in the screening of optical materials can be assumed by the dispersion. Fig. 5 demonstrates the dispersion spectra for the as prepared and irradiated Sb_2S_3 films. As one may observe from the plot, a normal dispersion (λ>600 nm) as well as an anomalous dispersion (λ<600 nm) with a single peak can be observed. Additionally, the strength of mono peak slightly increases as a consequence of irradiation with small shifting from their location. The increment of *n* by the irradiation might be ascribed to the adjustment in the material's density which is known as the irradiation affected refractive index changes. As such, these effects are alluring for the fabrication of diffractive optical elements (DOEs) or integrated optical components [25, 26].

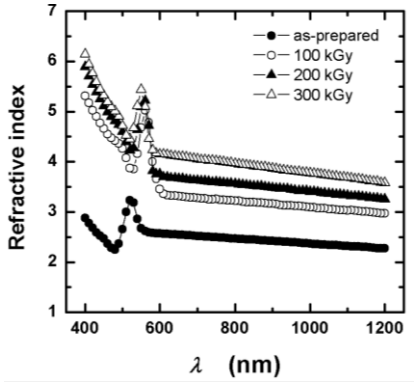

Fig. 5: The refractive index dispersion curves for as prepared and irradiated Sb_2S_3 films.

The optical dispersion of *n* at the normal incident is administered by the photon cooperation with the aggregate outermost electron shells originating from molecular arrangement structures. Along these lines, the investigation of the specific spectral regime has to give a light about the kind of clusters presented in the material gave that they supply a diverse number of electrons to their comparing outermost electron shells [27]. In the normal dispersion (λ>600 nm), the optical spectral behavior of the refractive index cab be modeled in accordance with the single oscillator model. The model connects the refractive index to the incident light frequency in the normal dispersion by the relation which confirmed by Wemple and DiDomenico [28,29]

$$n^2 - 1 = \frac{E_0 E_d}{E_o^2 - (h\nu)^2} \tag{9}$$

Here, E_o is the single oscillator energy of the optical transitions and E_d is the dispersion energy measuring the quality of interband transitions. Also, the modeling allowed explaining the dielectric reaction for transitions below the optical band gap. The slopes of the straight parts of the relation $(n^2\text{-}1)^{-1}\text{-}(h\nu)^2$ which is pictured in Fig. 6 reveal the oscillator and dispersion energies. E_o and E_d values were figured out and listed in Table 2. Additionally, the $(h\nu)^2$ - axis crossings of the straight lines ($(h\nu)^2 = 0$) that represent the best fits give the value of $n^2_\infty = \varepsilon_\infty$, which is computed and given in Table 2.

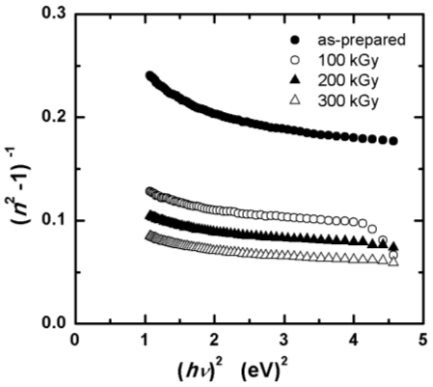

Fig. 6. The graph of $(n^2\text{-}1)^{-1}$ vs $(h\nu)^2$ for both as prepared and irradiated Sb_2S_3 films.

Table 2. The dispersion and nonlinear parameters of as prepared and irradiated Sb_2S_3 films

Sample	E_o (eV)	E_d (eV)	ε_∞	ε_L	N/m^* (10^{47} g^{-1} cm^{-3})	$\chi^{(3)}$ (10^{-11} esu)	n_2 (10^{-10} esu)
as-prepared	4.99	23.24	5.65	6.92	1.40	0.20	0.34
100 kGy	4.55	37.63	9.25	11.69	2.28	2.47	3.15
200 kGy	4.46	45.58	11.20	14.43	3.06	5.69	6.60
300 kGy	4.21	53.25	13.65	18.05	3.78	12.95	13.68

Furthermore, the index of refraction can be set out to write off the lattice dielectric consistent (ε_L), that depicts the lattice oscillation contribution and the dispersion of free carriers. In this work, we have assumed that the real part of the complex dielectric constant (ε_1) could be reproduced in term of the incident light wavelength (λ) in the normal dispersion part through the relation [22]:

$$\varepsilon_1 = n^2 = \varepsilon_L - \frac{e^2}{4\pi^2\varepsilon_o c^2}\frac{N}{m^*}\lambda^2 \tag{10}$$

Where e is the charge of electron, ε_o is the free space permittivity, c is the light speed and N/m^* is the ratio of concentration of free charge carriers to the free carrier effective mass. Fig. 7 displays the spectral dependence of n^2 (n^2vs. λ^2) for as prepared and irradiated Sb_2S_3 films. The real part of the complex dielectric constant ($\varepsilon_1=n^2$) at longer wavelengths exhibited a straight reliance. The slope of straight parts can be employed to evaluate the ratio N/m^*.Whilst, the values of the ε_L are given by extrapolating the straight portions to zero wavelengths. N/m^* and ε_L are tabulated in Table 2. As recorded in Table 2, the E_d,ε_∞, ε_L and N/m^* increase with excess of gamma does, while E_o decreases with excess of gamma doses. Such trend could be ascribed to the changes in bonds length at a degree relying upon the doses of gamma irradiation.

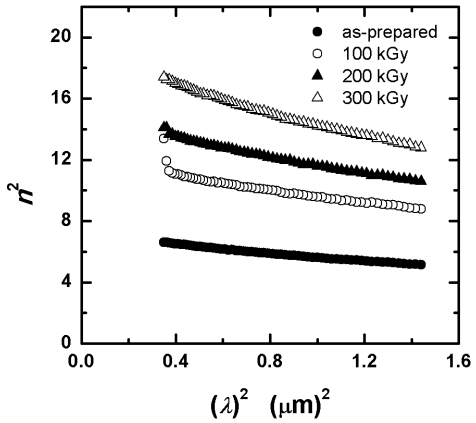

Fig. 7: The dependence of n^2 vs. λ^2 for as prepared and irradiated Sb_2S_3 films.

Third-order nonlinear optical susceptibility, $\chi^{(3)}$, is the expressing supposition of large variety of applications [30]. $\chi^{(3)}$ can be offered in accordance with Miller's principles through the equation [31]:

$$\chi^{(3)} = \frac{A(n_o^2-1)^4}{(4\pi)^4} \tag{11}$$

In this equation, A is a constant equal to 1.7×10^{-10} esu and the $\chi^{(3)}$ At the limit where there is zero photon energy ($n = n_o$). Wemple-DiDomenico static refractive index was combined with Miller's principles by Tichy *et al* [32]. Accordingly, the expression was employed to the nonlinear refractive index; n_2 is given by [31]:

$$n_2 = \frac{12\pi}{n_o}\chi^{(3)} \quad (12)$$

The evaluated values of $\chi^{(3)}$ and n_2 for Sb_2S_3 films are given in Table 2. It is found that $\chi^{(3)}$ and n_2 increased with increasing irradiation doses. This may be explained by that the external gamma irradiation causes an occurrence of defect centers, which may enhance local polarizabilities [32].

4. Conclusions

In present work we have investigated the impacts of the gamma irradiation on the properties of thermally evaporated Sb_2S_3 chalcogenide thin films. XRD showed that the Sb_2S_3 films have noncrystalline structure before and after irradiated. The variation trend of the optical bandgap could be filtered as far as the crystal mess resurgent and elevating number of disfigurement in crystal field and the structural bonding. The increment of the refractive index by the irradiation may be ascribed to the adjustment in the material's density known as the radiation affected refractive index changes. Such effectiveness is charming for the industry of diffractive optical components or conjoined optical portions. It is found that the nonlinear optical parameters increased with increasing irradiation doses. This may be due to the defect centers, which might modify local polarizabilities.

Acknowledgment

This work was supported by the Deanship of Scientific Research (DSR), King Abdulaziz University, Jeddah, under grant No. (363-122-D1436). The authors, therefore, gratefully acknowledge the DSR for technical and financial support.

References

[1] Y. R. EL-Mallawan, A. A. EL-Rahamani, Abousehl Y A., Yousef E., Mater. Chem. Phys. **161,** 52 (1998).
[2] K. Arshak, O. Korostynska, F. Fahim, Sensors **176,** 3 (2003).
[3] K. Arshak, O. Korostynska, Mater. Sci. Eng. B **224,** 107 (2004).
[4] M. M. EL-Nahass, A. A. A. Darwish, E. F. M. EL-Zaidia, A. E. Bekheet, J. Non-Cryst. Solids **382,** 74 (2013).
[5] M.M. EL-Nahass, K.F. Abd-EL-Rahman, H.M. Zeyada, A.A.A. Darwish, Opt. Commun. **285**, 2864 (2012).
[6] S.J. Moon, Y. Itzhaik, J.H. Yum, S.M. Zakeeruddin, G. Hodes, M. Grätzel, J. Phys. Chem. Lett. **1**, 1524 (2010).
[7] T. Fukumoto, T. Moehl, Y. Niwa, M.K. Nazeerddin, M. Grätzel, L. Etgar, Adv. Energy Mater. **3,** 29 (2013).
[8] M.Y. Versavel, J.A., Haber Thin Solid Films **515,** 7171 (2007).
[9] M. Kriisa, M. Krunks, I.O. Acik, E. Kärber, V. Mikli, Mater. Sci. Semicond. Process. **40**, 867 (2015).
[10] R. Boughalmi, A. Boukhachem, M. Kahlaoui, H. Maghraoui, M. Amlouk, Mater. Sci Semicond. Process. **26,** 593 (2014).
[11] P.A. Nwofe, Euro. J. Appl. Eng. Sci. Res. **4**, 1 (2015).
[12] M.C. Rodriguez, H. Martinez, Y. Peña, O. Flores, H.E.E. Ponce, A.S. Juarez, J.C. ALVarez, P. Reyes, Appl. Surf. Sci. **256,** 2428 (2010).
[13] K. F. Abd-EL-Rahman, A.A.A. Darwish, Current Appl. Phys. **11,** 1265 (2011).
[14] M. H. Lakhdar, B. Ouni, M. Amlouk, Mater. Sci. Semicond. Process. **19**, 32 (2014).

[15] F. Aousgi, W. Dimassi, B. Bessais, M. Kanzari, Appl. Surf. Sci. **350**, 19 (2015).
[16] S. Tolansky, Multiple-Beam Interference Microscopy of Metals, Academic Press, London, 1970.
[17] A.M. Bakry, A.H. EL-Naggar, Thin Solid Films, **360,** 293 (2000).
[18] A.H. EL- Naggar, J. Phys C: Condensed Matter, **11**, 9619 (1999).
[19] M.M. EL-Nahass, S. Yaghmour, Appl. Surf. Sci. **255**, 1631 (2008).
[20] R. Vijay, P.R. Babu, V.R. Kumar, M. Piasecki, D.K. Rao, N. Veeraiah, Mater. Sci. Semicond. Process. **35**, 96 (2015).
[21] S. Thomas, S.N. Rasool, M. Rathaiah, V. Nenkatramu, C. Joseph, N. Unnikrishnan, J. Non-Cryst. Solids **376,** 106 (2013).
[22] M.M. EL-Nahass, K.F. Abd-EL-Rahman, A.A.M. Farag, A.A.A. Darwish, Int. J. Mod. Phys. B **18,** 421 (2004).
[23] M.M. EL-Nahass, A.A. Atta, M.M. Abd EL-Raheem, A.M. Hassanien, J. Alloys Compd. **585**, 1 (2014).
[24] S.M. EL-Sayed, Nucl. Instrum. Methods Phys. Res. B **225,** 535 (2004).
[25] R.G. Hunsperger, Integrated Optics, Springer, Berlin, 1995.
[26] A. Yariv, Optical Electronics in Modern Communications, Oxford University Press, Oxford, 1997.
[27] J.M. Gonzalez-leal, J.A. Angel, E. Marquez, R. Jimenez-Garay, J. Phys. Chem. Solids **68**, 987 (2007).
[28] S.H. Wemple, M. J. Didomenco, Phys. Rev. B, **3,** 1338 (1971).
[29] S.H. Wemple, Phys. Rev. B, **7,** 3767 (1973).
[30] D. Cotter, R.J. Manning, K.J. Blow, A.D. Ellis, A.E. Kelly, D. Nesset, I.D. Phillips, A.J. Poustie, ROGERS D.C., Non Linear Opt. **286**, 1528 (1999).
[31] L. Tichý, H. Tichá, P. Nagels, R. Callaerts, R. Mertens, M. Vlček, Mater. Lett. **39,** 122 (1999).
[32] A.H. Medina, A.N. Mendoza, S.R. Bernal, G.S. Mejorada, J. Radioanal. Nucl. Chem. **286**, 643 (2010),.